

***c* , *e* and *d* waves detection in the acceleration photoplethysmogram**

Mohamed Elgendi

Department of Computing Science, University of Alberta, Canada
Tele: +1-780-807-4141
E-mail: moe.elgendi@gmail.com
URL: www.elgendi.net

Abstract

An efficient and robust method based on two moving average filters followed by a dynamic event duration threshold has been developed to detect *c* , *d* and *e* waves in the acceleration photoplethysmogram signals. The detection of *a* and *b* waves is affected by the quality of the photoplethysmogram recordings, especially for the heat stressed collection. The developed a method detects *a* and *b* waves in Arrhythmia APG Signals that suffer from: 1) non-stationary effects, 2) low signal-to-noise ratio, The performance of the proposed method was tested on 27 records collected in normal and heat-stressed conditions resulting in 99.95 percent sensitivity and 98.35 percent positive predictivity.

Keywords: acceleration photoplethysmogram, *c* wave detection, *d* wave detection, *e* wave detection, heat stress signal analysis

1. Introduction

It has been shown that atherosclerosis, the underlying cause of coronary heart disease, can occur even in children and adolescents. (Kimm et al.[1]; Strong et al. [2].; Leeson et al [3].). This fact leads to the belief that the primary prevention of atherosclerosis should commence in childhood. Monitoring arterial vascular walls as well as risk factors such as hypertension, hypercholesterolemia and other blood biochemical profiles can potentially help to identify individuals having an increased risk of developing atherosclerosis in adulthood.

Pulse-wave analysis has been shown to provide valuable information on aortic stiffness and elasticity (Chrife et al.[4]; Kelly et al.[5], O'Rourke et al.[6]), and it has been widely used to evaluate the vascular effects of aging, hypertension and atherosclerosis (Darne et al.[7]; Kelly et al.[8], Takazawa et al. [9]; Bortolotto et al.[10]).

Photoelectric plethysmography, also known as photoplethysmography and its acronym in some literature, is (PPG/PPG) and when it is called digital volume pulse, the acronym is (DVP). In this paper, the abbreviation PPG is going to be used according to Elgendi's recommendation [11].

Fingertip photoplethysmography mainly reflects the pulsatile volume changes in the finger arterioles, has been recognized as a noninvasive method of measuring arterial pulse waves in relation to changes in wave amplitude (Fichett [12]). However, the wave contour itself has not been analysed because of the difficulty in detecting minute changes in the phase of the

inflections. Previous attempts at PPG analysis showed that such delicate changes in the waves were emphasized and easily quantified by quadratically differentiating the original PPG signal with respect to time (Seki [13]; Ozawa [14]). Accordingly, the second derivative of the PPG (APG) was developed as a method allowing more accurate recognition of the inflection points and easier interpretation of the original plethysmogram wave. In this paper, the abbreviation APG for the second derivative photoplethysmogram will be used based on Elgendi's recommendation [11].

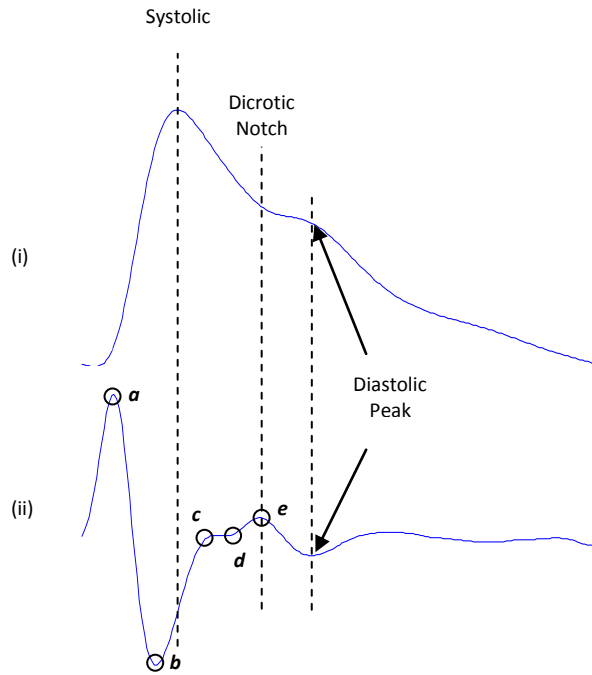


Figure 1 Signal Measurements [15] (i) fingertip photoplethysmogram (ii) second derivative wave of photoplethysmogram. The photoplethysmogram waveform consists of one systolic wave and one diastolic wave while the second derivative photoplethysmogram waveform consists of four systolic waves (*a*, *b*, *c*, and *d* waves) and one diastolic wave (*e* wave).

As shown in Figure 1, The waveform of the APG consists of four systolic waves (*a*, *b*, *c* and *d* waves) and one diastolic wave (*e* wave) Takazawa *et al.* [16]. The height of each wave was measured from the baseline, with the values above the baseline being positive and those under it negative.

This convenient and objective technique for analyzing the PPG wave has recently been performed more frequently than the conventional recordings. Several epidemiological studies have demonstrated that the information extracted from the APG waveform is associated closely with age and other risk factors for atherosclerotic vascular disease (Takada *et al.* [17]; Imanaga *et al.* [18]; Takazawa *et al.* [9]).

Takazawa *et al.* [19] demonstrated that the c/a ratio reflects decreased arterial stiffness, hence the c/a ratio decreases with age. The c/a index was also used by Šimek *et al.* (2005) [20] who found that the c/a index distinguishes subjects with essential hypertension from healthy controls. Baek *et al.* [21] found that the c/a ratio decreases with age just as the b/a ratio, described above. They also demonstrated that the d/a ratio reflects decreased arterial stiffness, hence the d/a ratio

decreases with age. Moreover, they found the $-d/a$ ratio is a useful index for the evaluation of vasoactive agents, as well as an index of left ventricular afterload. However, Baek *et al* [21] confirmed that the d/a ratios decreases with age.

Takazawa *et al.* [19] also found that the increase of the e/a ratio reflects decreased arterial stiffness, and that the e/a ratio decreases with age. Baek *et al* [21] confirmed that the e/a ratios decreases with age. Moreover, the $(b-c-d-e)/a$ index is useful for evaluating vascular aging and for screening of arteriosclerotic disease. Kimura *et al.* [22] calculated the vascular age as $45.5(b-c-d-e)/a + 65.9$ years old.

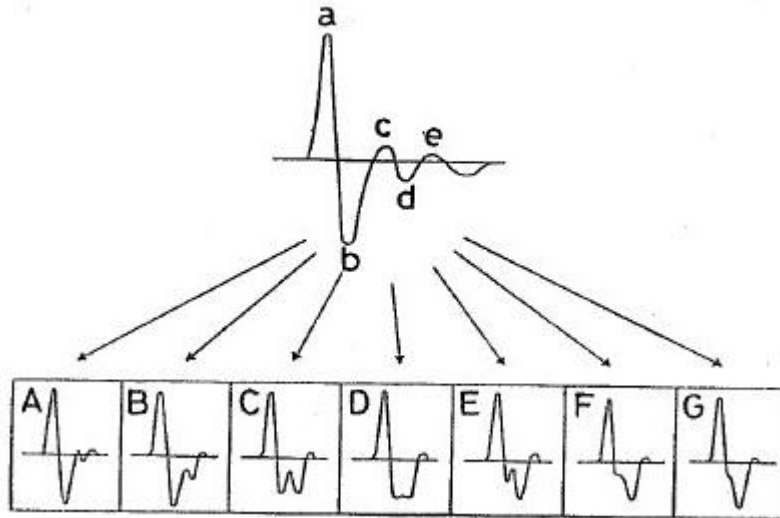


Figure 2 APG waveforms and types of photoplethysmogram [23]. There are different types of APG waveforms. The first APG waveform A (far left) refers to good circulation, whereas the amplitude of b wave is lower than c wave. The last APG waveform G (far right) refers to distinctively bad circulation, whereas the amplitude of c wave is lower than b wave.

Ushiroyama *et al.* [24] reported that patients with a sensation of coldness showed an improvement of the APG index $(b-c-d)/a$ upon treatment with a herbal supplement.

Another study by Sano *et al.* [25] proposed a more comprehensive aging index $(c+d-b)/a$ as it increases with age.

Homma *et al* succeeded in categorizing the APG into seven types depending on the waveforms, as shown in Figure 2. The clinical description of these categories has been demonstrated in Table 1.

Table 1 APG Wave Form Types [23]

Beat Type	Description
A	Good circulation
B	Good circulation but deteriorating
C	Poor circulation
D-G	Distinctively bad circulation

Although the clinical significance of APG measurement has been thoroughly discussed, there is still a lack of studies focusing on the automatic detection of c , d and e waves in APG signals.

Therefore this investigation, the first of its kind, aimed to develop a fast and robust algorithm to detect c , d and e waves in APG signals, especially in heat-stressed APG signal.

In literature, there are no studies that analyse or detect c , d and e waves. However, there was an attempt in 2009 by Matsuyama [26] to detect a waves in APG signals using nine QRS algorithms of Friesen's ECG algorithms [27] after modifying the sampling rates and threshold values. The detection rate was below 63 per cent for all nine algorithms when tested on the PPG-Army Heat Stress Dataset. Therefore, this investigation aims to develop a numerically efficient and robust algorithm to detect c , d and e waves in APG signals.

2. Data

There are currently no standard PPG databases available to evaluate the developed algorithms. However, Charles Darwin University has PPG dataset measured at rest and after exercise, as shown in Figure 3. Two independent annotators annotated a , b , c , d and e waves in APG signal.

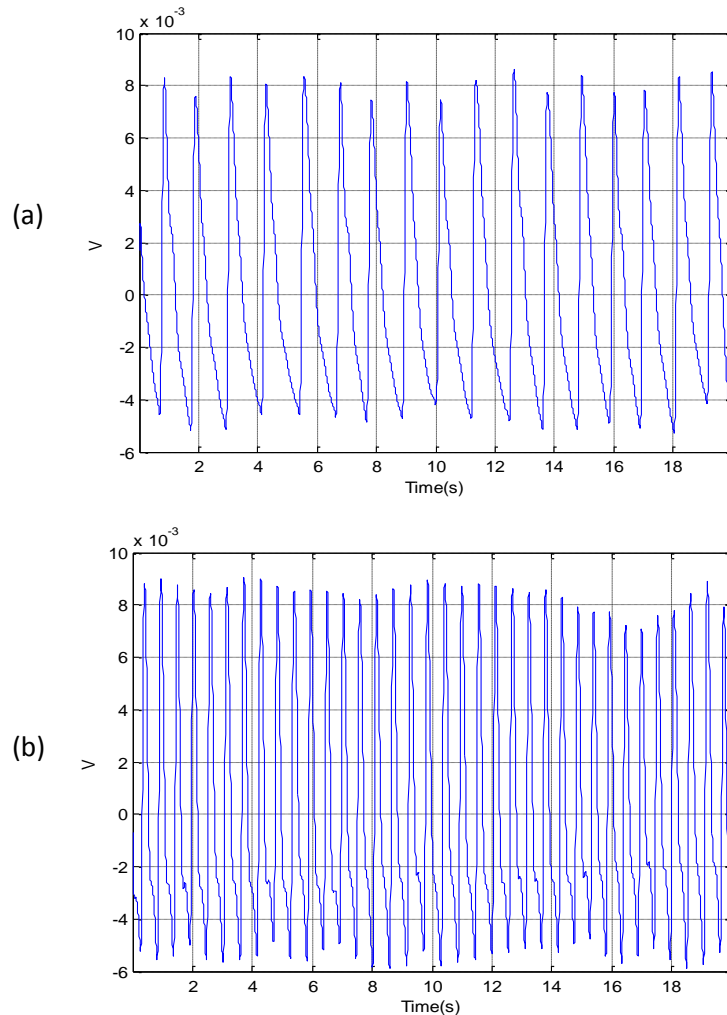


Figure 3 PPG signals: 20-seconds recording for the same volunteer, measured (a) at rest and (b) after exercise. It is clear that the heart rate after exercise is higher than at rest. This issue makes it challenging to detect heartbeats from APG signals.

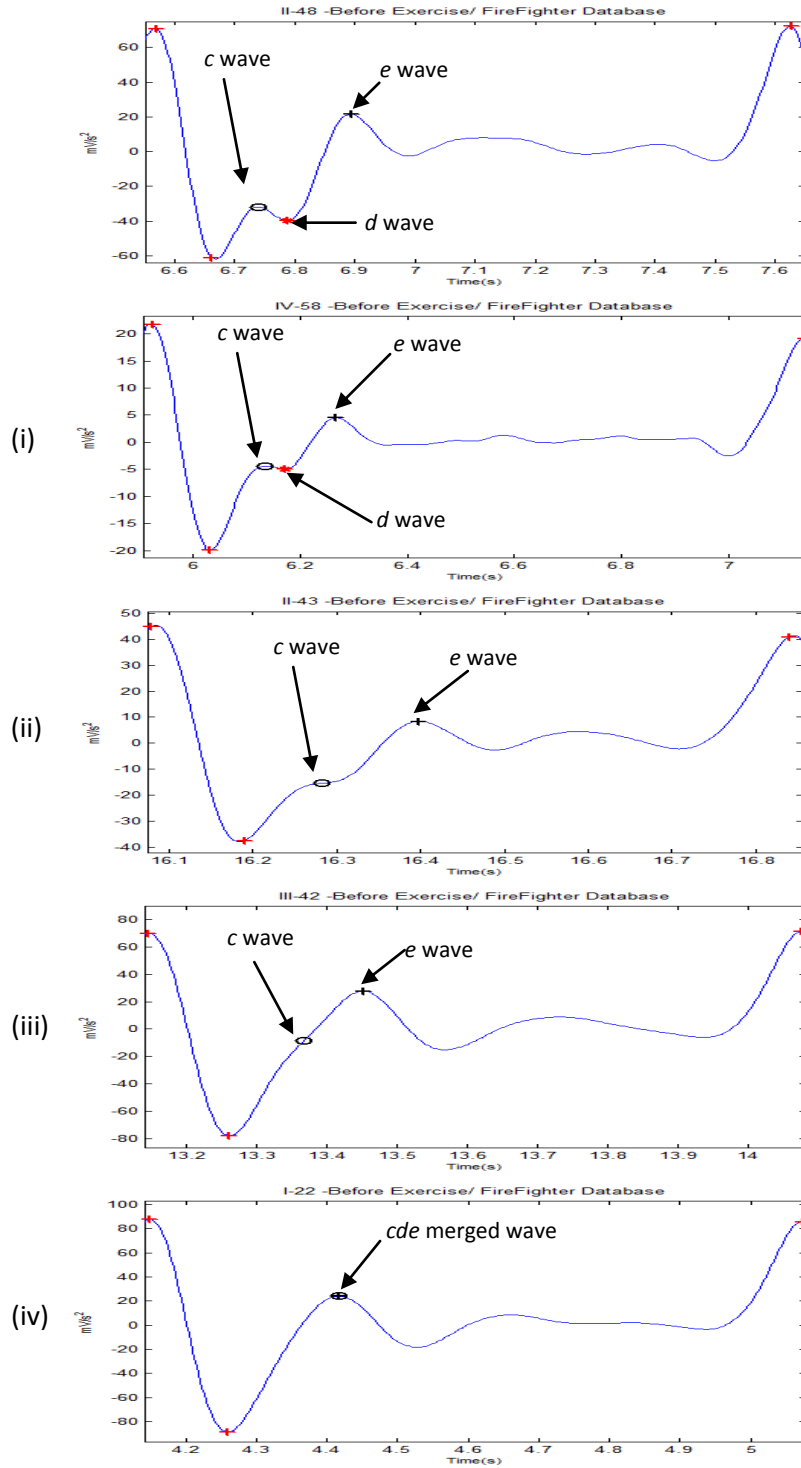


Figure 4 Annotation of *c*, *d*, and *e* waves (i) *c*, *d*, and *e* waves are salient (ii) *d* wave is not salient (iii) *d* wave is not salient (iv) *c*, *d*, and *e* waves are merged. The first two cases occur in the before-heat measurement while the last two cases are quite normal in the after-heat measurement of APG signals.

The PPG data were collected as a minor part of a joint project between Charles Darwin University, the Defence Science and Technology Organisation (DSTO) and the Department of Defence. The background of the entire project can be found in [26].

PPGs of 27 healthy volunteers (males) with a mean \pm SD age of 27 ± 6.9 were measured using a photoplethysmography device (Salus PPG), with the sensor located at the cuticle of the second digit of the left hand. Measurements were taken while the subject was at rest on a chair. PPG data were collected at a sampling rate of 200 Hz. The duration of each data segment is 20 seconds.

Annotation is a difficult task due to inter-annotator discrepancy, as the two annotators will never agree completely on what and how to annotate the c , d , and e wave. Despite the annotation process being significantly time-consuming, discrepancies can be found in many records. Three cases will be discussed below to show how the discrepancies were adjudicated:

❖ Case 1:

Annotator 1 agrees with Annotator 2 on all of the c , d , and e waves positions within an APG record. When both annotators have no discrepancies, it is an optimal situation.

❖ Case 2:

Both annotators agree on most of the c , d , and e waves positions.

❖ Case 3:

Annotator 2 considered the c , d , or e waves while Annotator 1 did not, and vice versa.

One annotation file has been saved to present the two annotated c , d , and e waves by considering the c , d , and e waves that have been missed by one of the annotators, or perhaps isolating d wave that is salient between c and e waves. The final consideration of c , d , and e waves will be based on the saliency of wave itself, as shown in Figure 4.

3. Methodology

The proposed c , e and d waves detection algorithm consists of three main stages: pre-processing (bandpass filtering, second derivative and squaring), feature extraction (generating potential blocks using two moving averages) and classification (thresholding). The structure of the algorithm is shown in Figure 5.

Bandpass Filter

To design an efficient bandpass filter, two types of challenging noise are addressed:

- i) **High-frequency noise:** this noise is could be due to the instrumentation amplifiers, the recording system pickup of ambient electromagnetic signals or other noises exist above 7 Hz, as shown in Figure 6 (a). High-frequency noise is usually caused by interference from mains power sources being induced onto the recording leads of the PPG. This phenomenon introduces a sinusoidal component into the recording. In Australia, this component is at a frequency of 50 Hz.
- ii) **Low-frequency noise:** this noise is created by poor contact to the fingertip photo sensor. In addition, variations in temperature and bias in the instrumentation amplifiers can cause baseline drift. Regarding the PPG databases used in this thesis, the body movement was limited due short measurement time (20 seconds) and the fixed position of the arm during the PPG signal collection.

The low-frequency noise can be removed using a high-pass filter. As shown in Figure 6 (b), the low frequencies that cause baseline wandering exist up to 0.5 Hz.

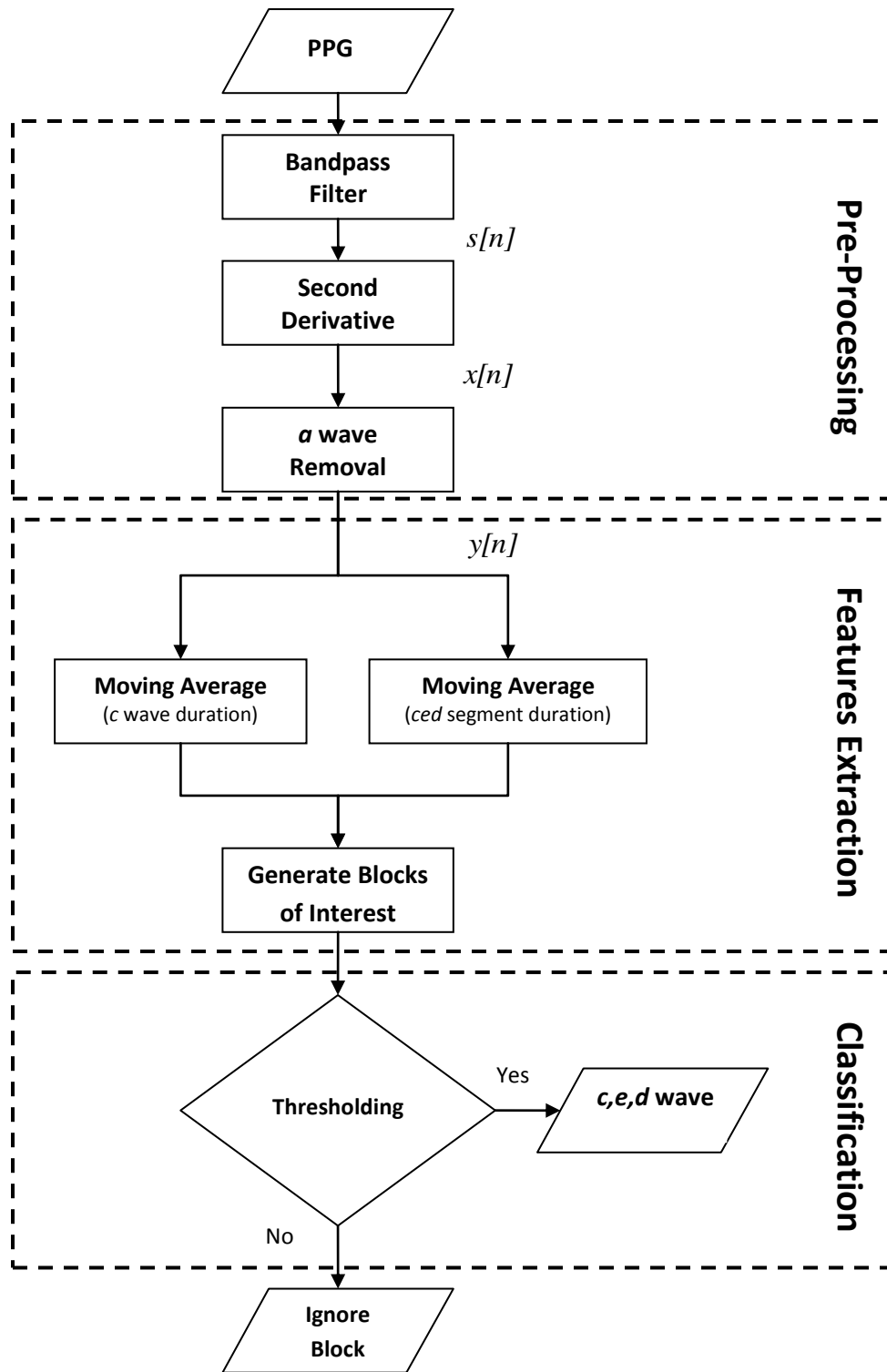


Figure 5 Flowchart for new *c*, *d*, and *e* wave detection algorithm. This *c*, *d*, and *e* waves algorithm is a time-domain algorithm that consists of three main stages: pre-processing, feature extraction and classification.

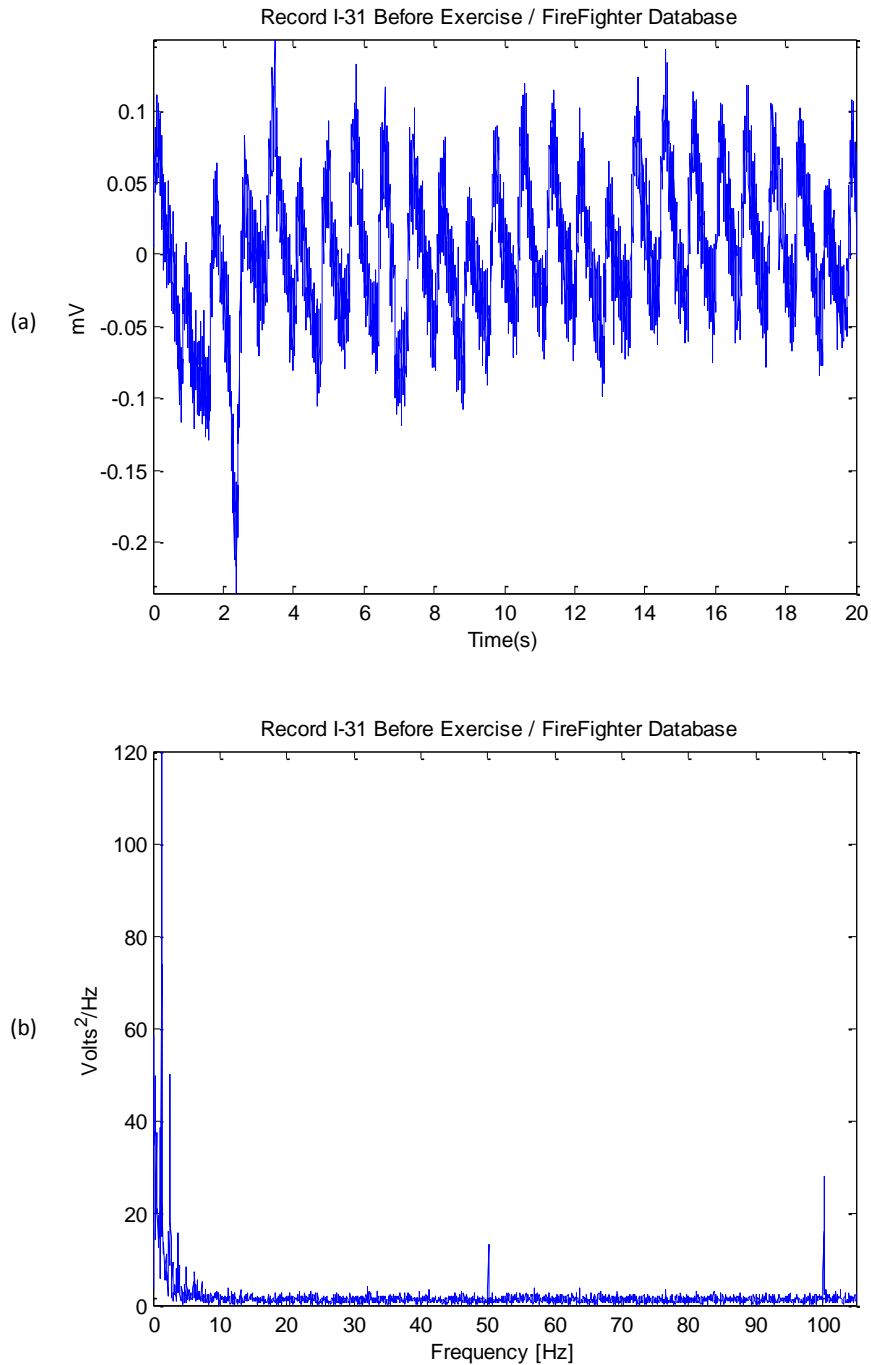


Figure 6 Demonstrating the PPG signals frequency bands (a) PPG signal, (b) Fourier transform (spectrum) of the PPG signal. The spectrum illustrates peaks at the fundamental frequency of 50 Hz, as well as the second and third harmonics at 100 Hz respectively. The spectrum shows that the main energy of the PPG signal lies up to 7 Hz.

The periodic interference is clearly displayed as a spike in Figure 6 (b) not only at its fundamental frequency of 50 Hz, but also as spikes at 100 Hz and the higher harmonics.

Extracting the main energy of a and b waves can be done using a bandpass filter which is typically a bidirectional Butterworth implementation [28], as it offers good transition-band characteristics at low coefficient orders making it efficient to implement [28].

A second-order Butterworth filter with bandpass 1–7 Hz has implemented by cascading a high- and low-pass filters to remove the baseline wander and high frequencies that do not contribute to the *a* and *b* waves. Since one complete heart cycle takes approximately one second, the frequencies below 1 Hz can be considered noise (baseline wander). The 7 Hz is chosen because most of the energy of the PPG signal is below 7 Hz, as shown in Figure 6 (b).

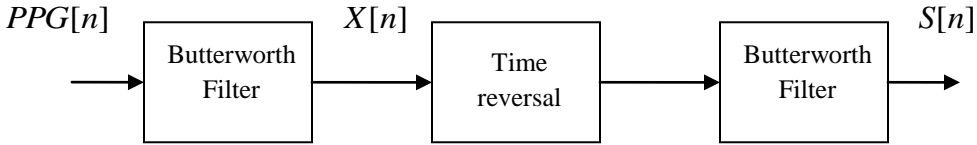


Figure 7 Demonstrating the zero-phase filtering in PPG signals

The bidirectional Butterworth filter is implemented as shown in Figure 7. The $S[n]$ output will be a filtered version of $PPG[n]$ with no phase distortion. The same Butterworth filter is used twice in this scheme: the time reversal step is a straight left–right flipping of the time-domain sequence, to produce zero-phase filtering, as follows:

$$X[n] = \sum_{k=0}^N b_k PPG[n-k] - \sum_{k=1}^N a_k X[n-k] \quad \text{Eq. 1}$$

$$S[n] = \sum_{k=0}^N b_k X[n-k] - \sum_{k=1}^N a_k S[n-k] \quad \text{Eq. 2}$$

Second Derivative

To obtain the APG signals $Z[n]$, the second derivative will be applied to the filtered PPG $S[n]$ in order to analyse the APG signals. Equations 3 and 4 represent a non-causal filter; the three-point centre derivative creates with a delay of only two samples.

$$S'[n] = \left. \frac{dS}{dt} \right|_{t=nT} = \frac{1}{2T} (S[n+1] - S[n-1]) \quad \text{Eq. 3}$$

$$Z[n] = \left. \frac{dS'}{dt} \right|_{t=nT} = \frac{1}{2T} (S'[n+1] - S'[n-1]) \quad \text{Eq. 4}$$

where T is the sampling interval and equals the reciprocal of the sampling frequency, and n is the number of data points. Figures 8 (a), 9 (a) and 10 (a) show the second derivative of the filtered PPG signal (APG signal) measured at rest and after exercise respectively.

b wave Cancellation

At this stage the a wave of the APG needs to be emphasised to distinguish it clearly for detection. This can be done by setting the negative parts of the signal equal to zero

```

IF  $Z[n] < 0$  THEN
     $Z[n] = 0$ 
END

```

a wave removal

To boost c and d waves to be dominant features in the APG signal, the a wave is removed. This is done by setting the $Z[n]$ signal to zero for the duration of the a wave, producing signal $y[n]$. Figures 8-10 (b) show the result of removing the a wave from the filtered signal of Figure 8-10 (a).

Generating blocks of interest

This methodology is based on Elgendi's methodology [29-32] in detecting a and b waves in APG signals using two moving averages. However, in here the c , d , e waves will be detected instead of a wave. Thus, the duration of the first moving average will be related to the minimum duration of the c , d , e waves which is about 8 ms while the duration of the second moving average will be related the average length of the ced segment which is about 40 ms, as follows:

i) First Moving Average: the first moving average, shown as the dotted line in Figures 8-10 (b), is used to detect the peaks of c and d waves.

$$MA_{Peak}[n] = \frac{1}{W_1} (y[n - (W_1 - 1)/2] + \dots + y[n] + \dots + y[n + (W_1 - 1)/2]) \quad \text{Eq. 5}$$

where $W_1 = 8 \text{ ms} * SF$, which is the average duration for c , d , and e wave, is rounded to the nearest odd integer.

ii) Second moving average: is used as a threshold for the first moving average, and is shown as a solid line in Figures 8-10 (b).

$$MA_{CED\text{Segment}}[n] = \frac{1}{W_2} (y[n - (W_2 - 1)/2] + \dots + y[n] + \dots + y[n + (W_2 - 1)/2]) \quad \text{Eq. 6}$$

where $W_2 = 40 \text{ ms} * SF$, which is the average duration for the ced segment, is rounded to the nearest odd integer.

When the amplitude of the first moving-average filter (MA_{Peak}) is greater than the amplitude of the second moving-average filter ($MA_{CED\text{segment}}$), the blocks of interest will be generated as follows:

```

IF  $MA_{Peak}[n] > MA_{CED\text{segment}}[n]$  THEN
     $Blocks[n] = 1$ 
ELSE
     $Blocks[n] = 0$ 
END

```

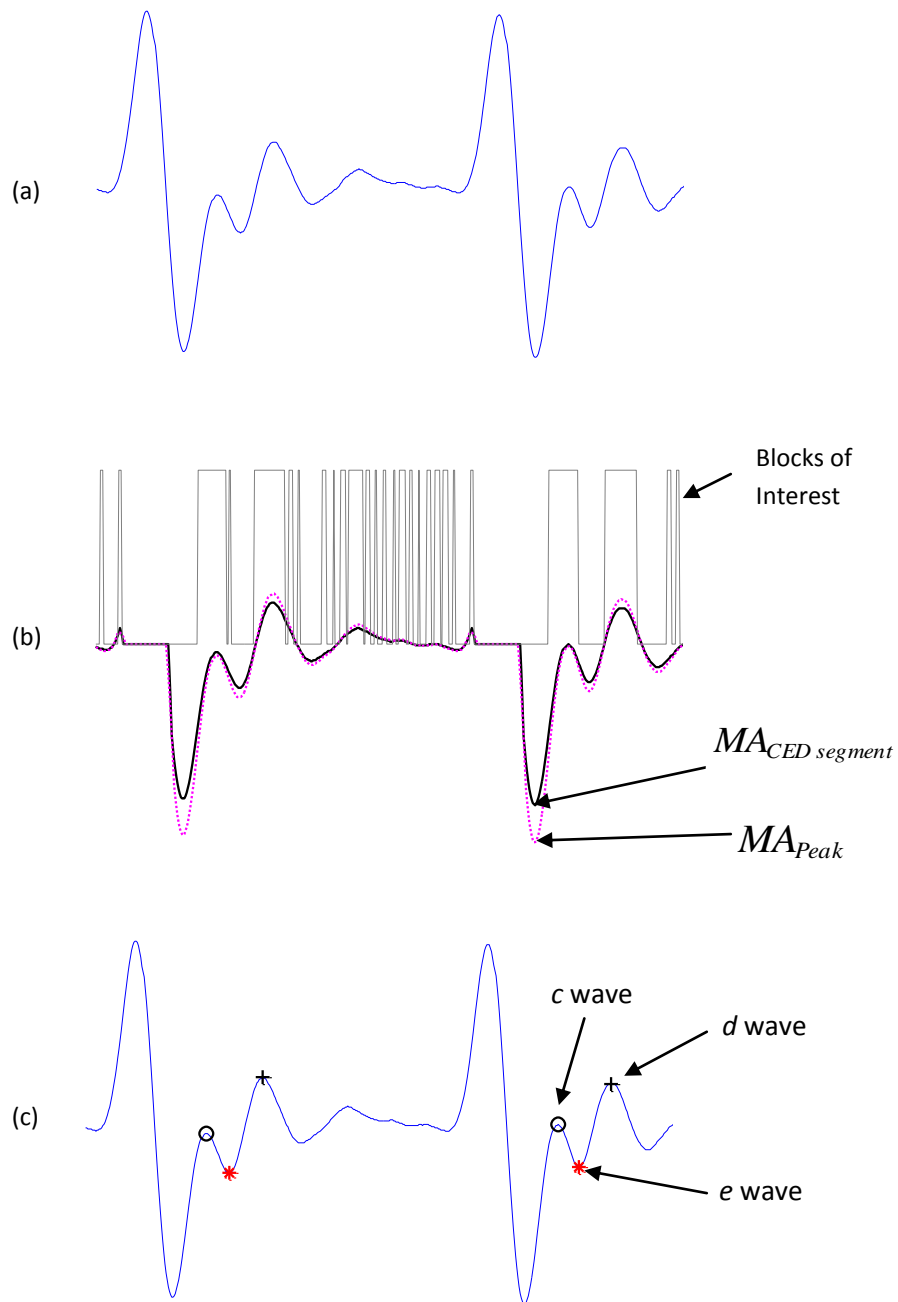


Figure 8 Case 1: Demonstrating the effectiveness of using two moving averages to detect *c*, *d* and *e* waves (a) filtered APG signal with Butterworth bandpass filter (b) generating blocks of interest after using two moving averages: the dotted line is the first moving average and the solid line is the second moving average (c) the detected *c*, *d* and *e* waves after applying the thresholds.

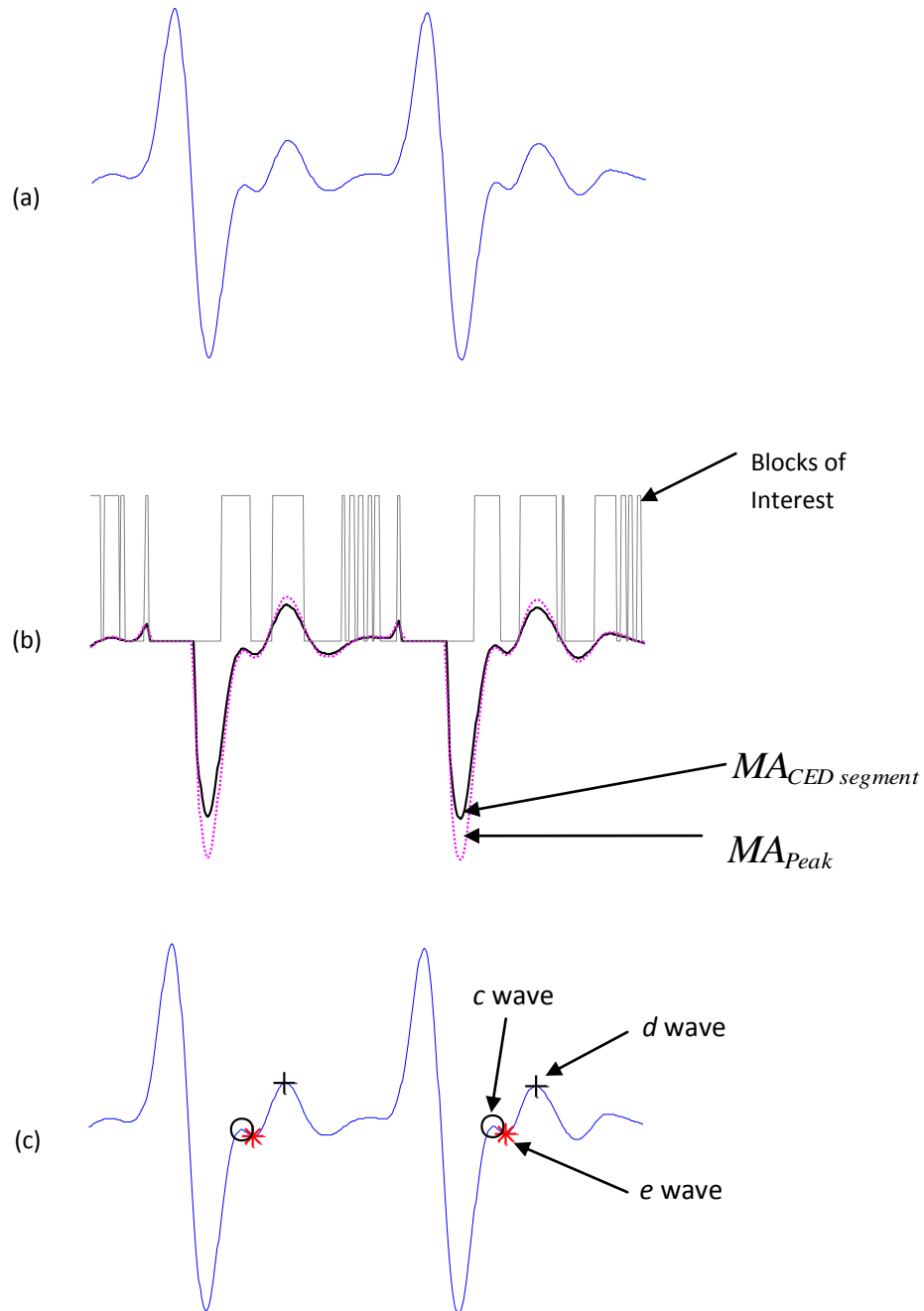


Figure 9 Case 2: Demonstrating the effectiveness of using two moving averages to detect *c*, *d* and *e* waves. (a) filtered APG signal with Butterworth bandpass filter, (b) generating blocks of interest after using two moving averages: the dotted line is the first moving average and the solid line is the second moving average, (c) the detected *c*, *d* and *e* waves after applying the thresholds.

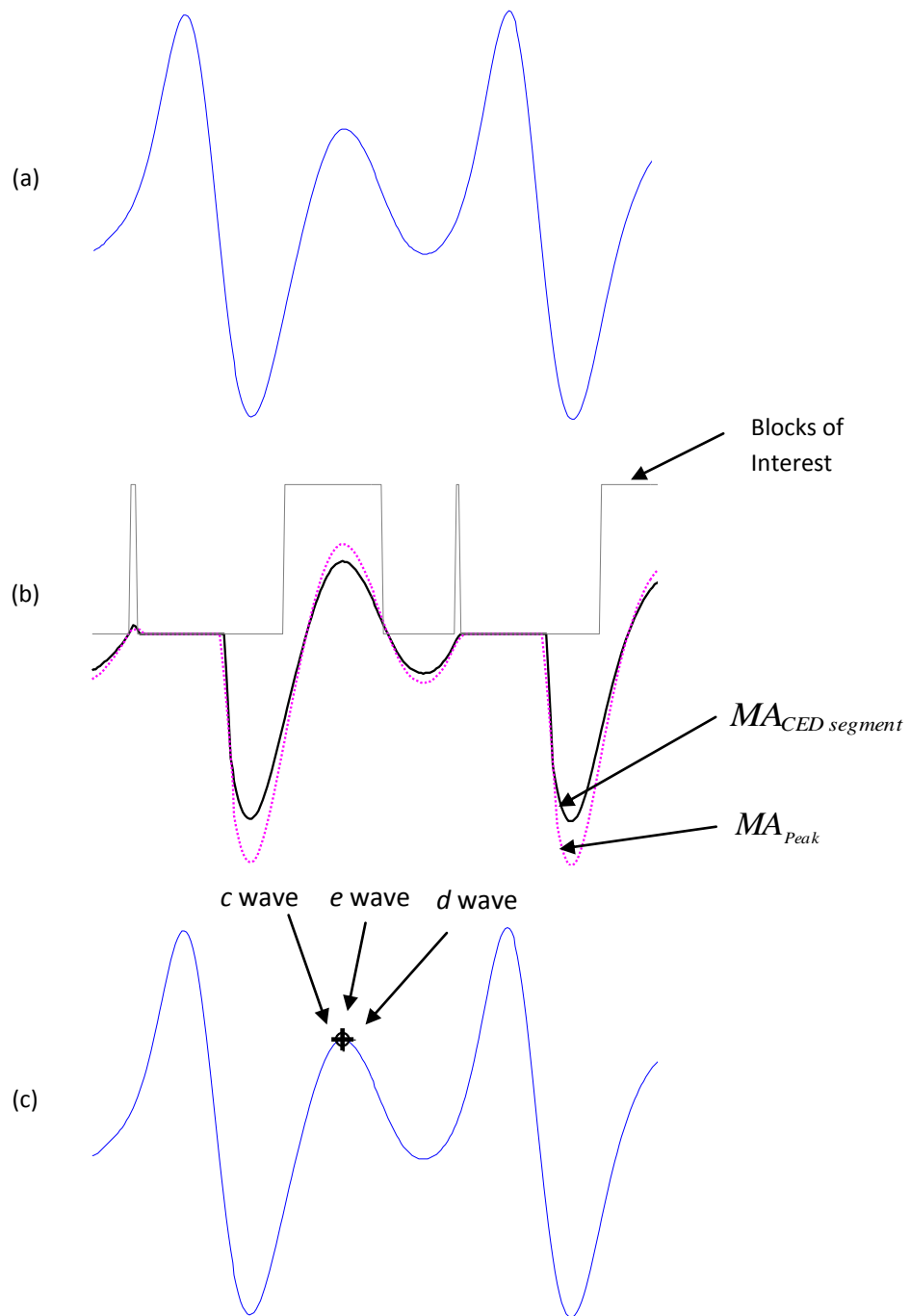


Figure 10 Case 3: Demonstrating the effectiveness of using two moving averages to detect *c*, *d* and *e* waves. (a) Filtered APG signal with Butterworth bandpass filter, (b) generating blocks of interest after using two moving averages: the dotted line is the first moving average and the solid line is the second moving average, (c) the detected *c*, *d* and *e* waves after applying the thresholds.

Thresholding

Blocks with a smaller width than the average window size of the c , d or e peak (W_I) are considered noisy blocks and rejected. The expected size for the c , d or e peak is based on observational statistics for healthy adults, which varies from 6 ms to 10ms.

$$peak_Block\ size = (a_i a_{i+1} / SF) * W_I \quad \text{Eq. 7}$$

where $a_i a_{i+1}$ is the aa interval that contains the blocks of interest and SF is the sampling frequency.

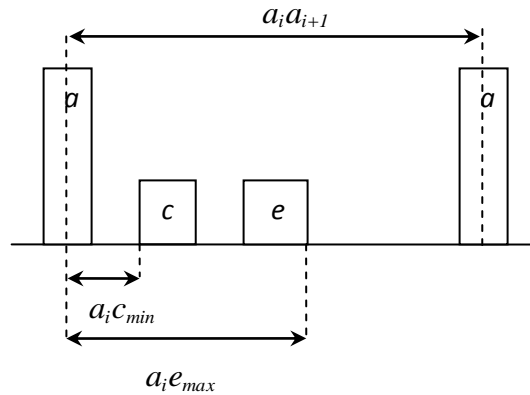


Figure 11 Demonstrating c , d and e waves time occurrence regarding the current a peak and the next a peak. Where $a_i c_{min}$ represents the minimum interval between the c wave and the current a peak while, $a_i e_{max}$ represents the maximum interval between the e wave and the current a peak.

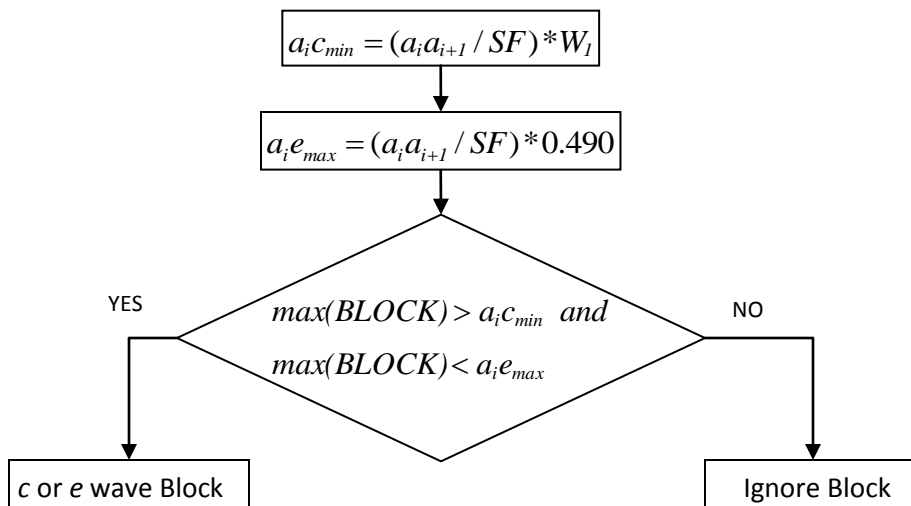


Figure 12 Flowchart for selection of c and e waves.

In order to determine whether the detected blocks contain c , d or e waves, the number of blocks in each consecutive aa interval is first counted. A threshold is then applied based on the distance of the maximum point within a block to the a peak to distinguish c waves from e waves and noise.

There are three possibilities for the number of detected blocks:

1. More than one block: the distance of the maximum point within a block to the nearest a peak will be used as a measure for selecting the blocks that contain potential c , e or d waves. This consists of two steps:
 - i. *Detect potential c and e waves.* a block will be considered as containing a c wave if the distance of the maximum point of the block to the nearest a peak is within a certain range as shown in Figures 11-12. The maximum absolute value within the first accepted block at the right-hand-side of the b wave is considered the c peak. The maximum absolute value of the second accepted block after the c peak is considered the e peak. Usually the c , e , and d waves do exist in APG signals measured at rest as shown in Figure 13 (a,d).
 - ii. *Detect d waves.* the minimum value that lies between the c peak and the e peak is considered the d peak, as shown in Figures 8-10 (c).
2. One block: the c and e waves are most likely merged within one block, which is marked with a \oplus symbol, as shown in Figure 10 (c). The c , e , and d waves are usually merged in APG signals measured after exercise, as shown in Figure 14.

The detected waves were compared to the annotated waves, discussed in Appendix C, to determine whether the c , d , and e waves were detected correctly.

The following statistical parameters were used to evaluate the algorithm:

$$Se_{c/d/e} = \frac{TP_{c/d/e}}{TP_{c/d/e} + FN_{c/d/e}} \quad \text{Eq. 8}$$

$$+ P_{c/d/e} = \frac{TP_{c/d/e}}{TP_{c/d/e} + FP_{c/d/e}} \quad \text{Eq. 9}$$

- **If c , d and e waves exist, the statistical parameters will be defined as:**
 - True Positive ($TP_{c/d/e}$): the $c/d/e$ wave has been classified as the $c/d/e$ wave, as shown in Figure 13 (a,b,d).
 - *With high heart rates, the d wave does not exist or may be smoothed [26]. In this case, the true positives will be defined as:
 - True Positive (TP_d): the d wave does not exist and the algorithm did not detect it, as shown in Figure 13 (c).
 - False Negative ($FN_{c/d/e}$): the $c/d/e$ wave has not been classified as the $c/d/e$ wave.
 - False Positive ($FP_{c/d/e}$): the non- $c/d/e$ wave has been classified as the $c/d/e$ wave.
- **If c , d and e waves are merged, the statistical parameters will be defined as:**
 - True Positive ($TP_{c,d,e}$): merged c , d and e waves has been classified as merged c , d and e waves (see Figure 14 (a-c)) , regardless of the location of merging [26].
 - False Negative ($FN_{c,d,e}$): merged c , d and e waves have not been classified as merged c , d and e waves.
 - False Positive ($FP_{c,d,e}$): non-merged c , d and e waves have been classified as merged c , d and e waves.

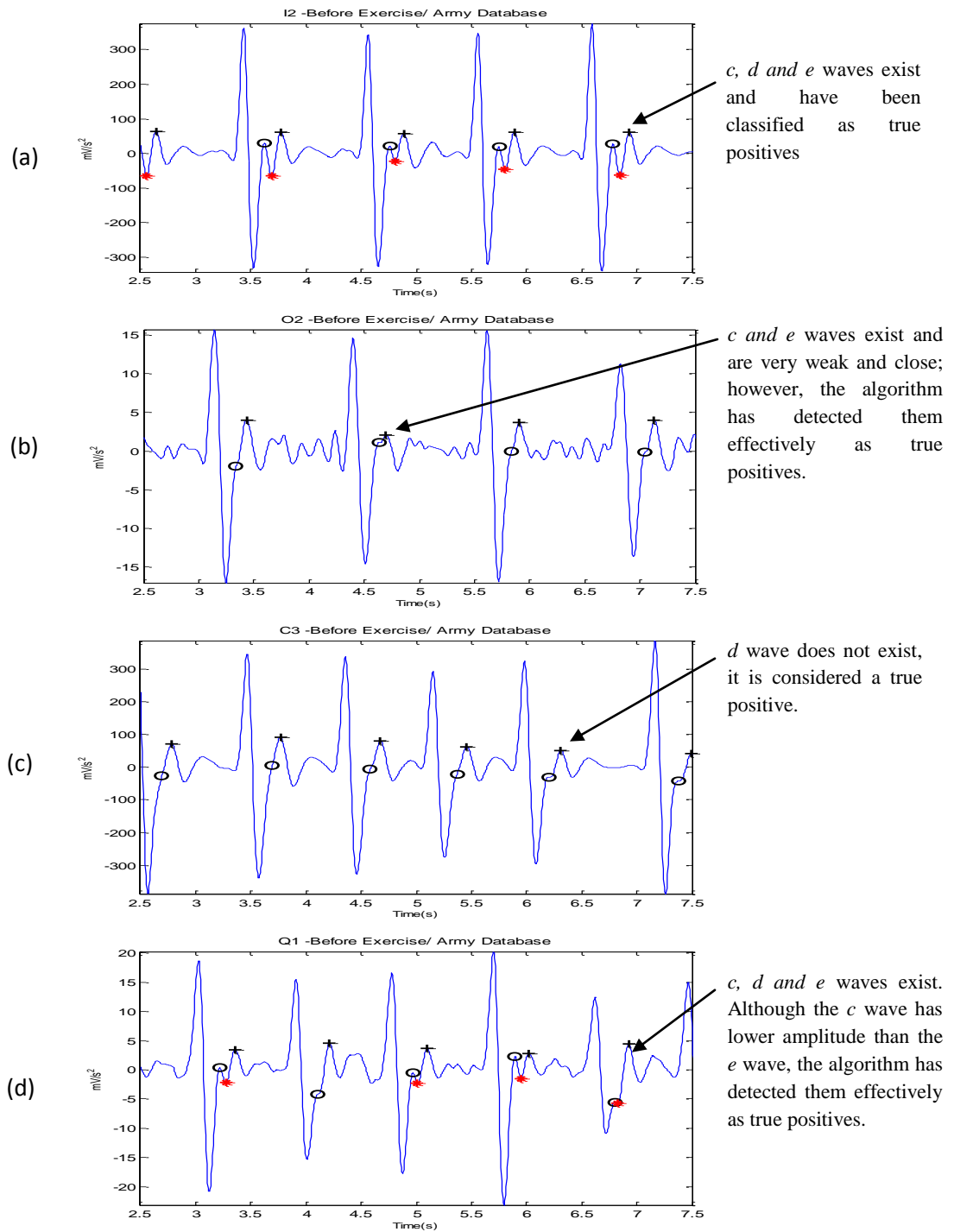


Figure 13 Detected *c*, *e* and *d* waves in APG signals before exercise. This contains (a) stationary signals, (b) low amplitudes, (c) irregular heart rhythm, (d) high frequency noise. 'O' represents the *c* wave, '+' represents the *d* wave and '*' represents the *e* wave.

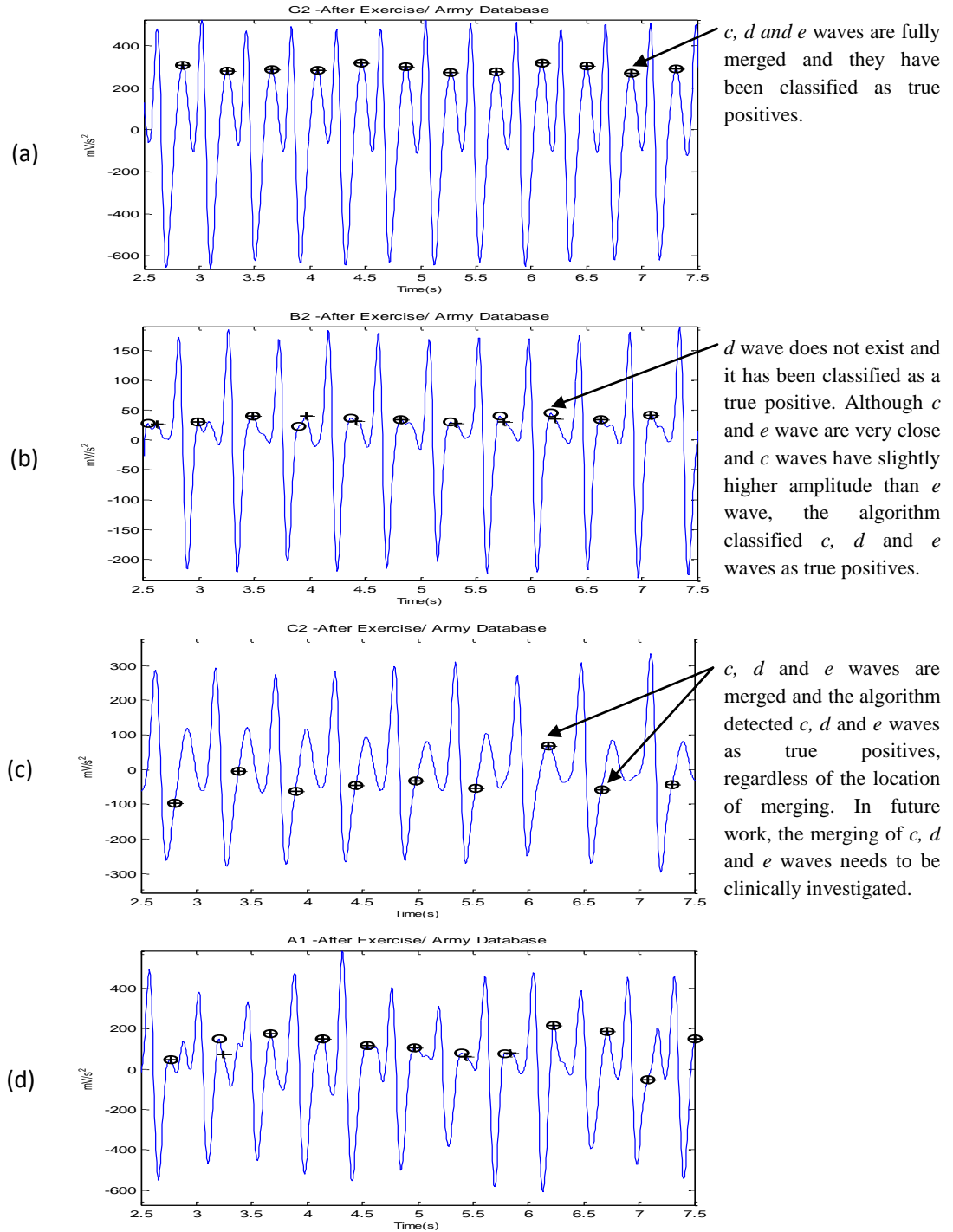


Figure 14 Detected *c*, *e* and *d* waves in APG signals after exercise. This contains (a) stationary signals, (b) low amplitudes, (c) irregular heart rhythm, (d) high-frequency noise. ‘O’ represents the *c* wave, ‘+’ represents the *e* wave, and ‘ \oplus ’ represents the merged *c*, *e*, and *d* waves.

Table 2 c wave detection performance on the PPG-Army Database

Record	Before exercise						After exercise					
	No of beats	TP	FP	FN	Se (%)	+P (%)	No of beats	TP	FP	FN	Se (%)	+P (%)
A1	26	26	0	0	100.0	100.0	45	45	0	0	100.0	100.0
A2	24	23	1	0	100.0	95.8	44	39	5	0	100.0	88.6
B1	17	17	0	0	100.0	100.0	36	35	1	0	100.0	97.2
B2	26	25	1	0	100.0	96.2	43	42	1	0	100.0	97.7
C2	20	20	0	0	100.0	100.0	33	32	1	0	100.0	97.0
C3	20	20	0	0	100.0	100.0	30	28	1	0	100.0	96.6
D2	22	21	1	0	100.0	95.5	33	28	5	0	100.0	84.8
D3	19	19	0	0	100.0	100.0	23	23	0	0	100.0	100.0
E1	22	22	0	0	100.0	100.0	25	24	1	0	100.0	96.0
E2	22	22	0	0	100.0	100.0	25	24	1	0	100.0	96.0
E3	19	19	0	0	100.0	100.0	34	32	2	0	100.0	94.1
G2	30	28	2	0	100.0	93.3	48	48	0	0	100.0	100.0
G3	19	19	0	0	100.0	100.0	33	31	2	0	100.0	93.9
H3	23	22	1	0	100.0	95.7	31	31	0	0	100.0	100.0
I1	22	22	0	0	100.0	100.0	30	28	2	0	100.0	93.3
I2	17	17	0	0	100.0	100.0	28	26	2	0	100.0	92.9
J2	23	22	1	0	100.0	95.7	36	35	1	0	100.0	97.2
L2	24	24	0	0	100.0	100.0	36	36	0	0	100.0	100.0
L3	24	24	0	0	100.0	100.0	35	33	2	0	100.0	94.3
N2	18	18	0	0	100.0	100.0	23	23	0	0	100.0	100.0
N3	20	20	0	0	100.0	100.0	29	29	0	0	100.0	100.0
O1	24	24	0	0	100.0	100.0	29	29	0	0	100.0	100.0
O2	17	17	0	0	100.0	100.0	32	26	6	0	100.0	81.3
P1	26	26	0	0	100.0	100.0	35	33	2	0	100.0	94.3
P2	20	20	0	0	100.0	100.0	29	29	0	0	100.0	100.0
Q1	22	22	0	0	100.0	100.0	27	26	1	0	100.0	96.3
Q2	18	18	0	0	100.0	100.0	33	33	0	0	100.0	100.0
²⁷ volunteers	584	577	7	0	100.0	98.97	885	848	36	0	100.0	95.98

Table 3 d wave detection performance on the PPG-Army Database

Record	Before exercise						After exercise					
	No of beats	TP	FP	FN	Se (%)	+P (%)	No of beats	TP	FP	FN	Se (%)	+P (%)
A1	26	26	0	0	100.0	100.0	45	45	0	0	100.0	100.0
A2	24	24	0	0	100.0	100.0	44	44	0	0	100.0	100.0
B1	17	17	0	0	100.0	100.0	36	36	0	0	100.0	100.0
B2	26	26	0	0	100.0	100.0	43	43	0	0	100.0	100.0
C2	20	18	2	0	100.0	90.0	33	33	0	0	100.0	100.0
C3	20	19	1	0	100.0	95.0	30	30	0	0	100.0	100.0
D2	22	22	0	0	100.0	100.0	33	33	0	0	100.0	100.0
D3	19	19	0	0	100.0	100.0	23	21	2	0	100.0	91.3
E1	22	22	0	0	100.0	100.0	25	24	1	0	100.0	96.0
E2	22	22	0	0	100.0	100.0	25	24	1	0	100.0	96.0
E3	19	19	0	0	100.0	100.0	34	34	0	0	100.0	100.0
G2	30	30	0	0	100.0	100.0	48	48	0	0	100.0	100.0
G3	19	19	0	0	100.0	100.0	33	32	1	0	100.0	97.0
H3	23	22	1	0	100.0	95.7	31	28	3	0	100.0	90.3
I1	22	22	0	0	100.0	100.0	30	30	0	0	100.0	100.0
I2	17	17	0	0	100.0	100.0	28	28	0	0	100.0	100.0
J2	23	23	0	0	100.0	100.0	36	36	0	0	100.0	100.0
L2	24	23	1	0	100.0	95.8	36	36	0	0	100.0	100.0
L3	24	24	0	0	100.0	100.0	35	35	0	0	100.0	100.0
N2	18	17	1	0	100.0	94.4	23	23	0	0	100.0	100.0
N3	20	19	1	0	100.0	95.0	29	27	2	0	100.0	93.1
O1	24	24	0	0	100.0	100.0	29	29	0	0	100.0	100.0
O2	17	16	1	0	100.0	94.1	32	32	0	0	100.0	100.0
P1	26	21	5	0	100.0	80.8	35	35	0	0	100.0	100.0
P2	20	20	0	0	100.0	100.0	29	29	0	0	100.0	100.0
Q1	22	22	0	0	100.0	100.0	27	27	0	0	100.0	100.0
Q2	18	18	0	0	100.0	100.0	33	33	0	0	100.0	100.0
27 volunteers	584	571	13	0	100.0	97.81	885	875	10	0	100.0	98.66

Table 4 *e* wave detection performance on the PPG-Army Database

Record	Before exercise						After exercise					
	No of beats	TP	FP	FN	Se (%)	+P (%)	No of beats	TP	FP	FN	Se (%)	+P (%)
A1	26	26	0	0	100.0	100.0	45	45	0	0	100.0	100.0
A2	24	24	0	0	100.0	100.0	44	39	5	0	100.0	88.6
B1	17	17	0	0	100.0	100.0	36	36	0	0	100.0	100.0
B2	26	26	0	0	100.0	100.0	43	41	2	2	95.3	95.3
C2	20	20	0	0	100.0	100.0	33	32	1	0	100.0	97.0
C3	20	20	0	0	100.0	100.0	30	29	0	0	100.0	100.0
D2	22	22	0	0	100.0	100.0	33	33	0	0	100.0	100.0
D3	19	19	0	0	100.0	100.0	23	23	0	0	100.0	100.0
E1	22	22	0	0	100.0	100.0	25	25	0	0	100.0	100.0
E2	22	22	0	0	100.0	100.0	25	25	0	0	100.0	100.0
E3	19	19	0	0	100.0	100.0	34	34	0	0	100.0	100.0
G2	30	30	0	0	100.0	100.0	48	48	0	0	100.0	100.0
G3	19	19	0	0	100.0	100.0	33	33	0	0	100.0	100.0
H3	23	21	2	0	100.0	91.3	31	31	0	0	100.0	100.0
I1	22	22	0	0	100.0	100.0	30	30	0	0	100.0	100.0
I2	17	17	0	0	100.0	100.0	28	28	0	0	100.0	100.0
J2	23	23	0	0	100.0	100.0	36	36	0	0	100.0	100.0
L2	24	24	0	0	100.0	100.0	36	36	0	0	100.0	100.0
L3	24	24	0	0	100.0	100.0	35	35	0	0	100.0	100.0
N2	18	18	0	0	100.0	100.0	23	22	1	0	100.0	95.7
N3	20	20	0	0	100.0	100.0	29	28	1	1	96.6	96.6
O1	24	24	0	0	100.0	100.0	29	29	0	0	100.0	100.0
O2	17	17	0	0	100.0	100.0	32	32	0	0	100.0	100.0
P1	26	26	0	0	100.0	100.0	35	35	0	0	100.0	100.0
P2	20	20	0	0	100.0	100.0	29	29	0	0	100.0	100.0
Q1	22	22	0	0	100.0	100.0	27	27	0	0	100.0	100.0
Q2	18	18	0	0	100.0	100.0	33	33	0	0	100.0	100.0
27 volunteers	584	582	2	0	100.0	99.68	885	874	10	3	99.70	99.01

Discussion and Conclusion

The proposed algorithm was tested on the PPG-Army dataset. As mentioned in Chapter 4, this dataset contains 27 APG recordings measured before and after exercise. The main objective behind testing the algorithm against the APG measured after exercise is to test the robustness of the algorithm against non-stationary effects, low SNR, and high heart rate. All of the reasons for detection failure are described below.

- 1) **Stationarity.** the APG signals for volunteers I2 -before exercise and G2 (after exercise) are stationary. The proposed algorithm detected the *c*, *d*, and *e* waves correctly in stationary APG signals as shown in Figure 13 (a). In Figure 14 (a), the *c*, *d*, and *e* waves are merged because of the high heart rate of the subject.
- 2) **Low Amplitude.** the APG signals of volunteers O2 (before exercise) and B2 (after exercise) have low amplitude. The proposed algorithm handled very poor amplitudes, as shown in Figures 13 (b) and 14 (b).
- 3) **Non-Stationarity.** the proposed algorithm detected the *c*, *d*, and *e* waves correctly in non-stationary APG signals as shown in Figures 13 (c,d) and 14 (c,d).
- 4) **Regular Heart Rhythm.** the proposed algorithm detected the *c*, *d*, and *e* waves correctly in APG signals with regular heart rhythms as shown in Figures 12 (a,b,d) and 13 (a ,b, d).
- 5) **Irregular Heart Rhythm.** Figures 13 (c) and 14 (c) have irregular rhythms and the *c*, *d*, and *e* waves have been detected successfully. Figure 13 (c) shows that *d* wave is smoothed with *c* and *e* waves; after exercise (or high heart rate), the *d* wave usually vanishes and the *c*, *d* and *e* waves are merged.
- 6) **High Frequency Noise.** as shown in Figures 13 (d) and 14 (d), the proposed algorithm is very robust to noise, for volunteers Q1 (before exercise) and A1(after exercise).

Although the duration of *c*, *d* and *e* waves changed dramatically after exercise, the proposed algorithm succeeded in detecting the *c*, *d* and *e* waves efficiently as shown in Tables 2-4.

Few false negative occur in N3 and B2 subjects measured after exercise, this is because *e* wave was not salient enough to be detected, about to merge with *c* and *d* waves. Due to high noise the APG signals, a number of false positives occurred. However, the number of false positives in the detection of *c* waves was the highest because of its morphology and small duration.

Most research relating to the APG has been done in Japan. In addition to cardiovascular risk factors, the APG has also been described as a potential diagnostic tool for other disorders, varying from a sensation of coldness and stress experienced by surgeons to exposure to lead, pneumonia, intracerebral haemorrhage and acute poisoning.

Currently a full understanding of the diagnostic value of the different features of the PPG signal is still lacking and more research is needed. Moreover, the detection algorithm of *c*, *d* and *e* waves in APG signals can hardly be found in literature.

However, a promising algorithm has been proposed to detect *c*, *d* and *e* waves simultaneously and robustly against high-frequency noise, low amplitude, non-stationary effects and irregular heartbeats in APG signals measured before and after exercise. This numerically-efficient algorithm was evaluated using 27 records, containing 1,469 heartbeats resulting in 99.95 percent sensitivity and 98.35 percent positive predictivity.

The accurate detection of *c*, and *d* and *e* waves in the APG offers a non-invasive method of evaluating cardiac functioning and identifying individuals at risk.

Acknowledgement

Mohamed Elgendi would like to gratefully acknowledge the Australian government and Charles Darwin University whose generous scholarships facilitated this research. He would like also to thank Prof. Friso De Boer and Mrs. Mirjam Jonkman for their valuable comments and annotation of the used dataset. He also would like to thank Dr Gari Clifford for helpful discussions.

References

1. Kimm SY, P.G., Stylianou MP, Waclawiw MA, Lichtenstein C *National trends in the management of cardiovascular disease risk factors in children: second NHLBI survey of primary care physicians.* Pediatrics, 1998: 102:E50.
2. Strong JP, M.G., McMahan CA, Tracy RE, Newman WP, Herderick EE, Cornhill JF . *Prevalence and extent of atherosclerosis in adolescents and young adults. Implications for prevention from the pathobiological determinants of atherosclerosis in young study.* JAMA 1999: 281:727-737.
3. Leeson CP, W.P., Cook DG, Mullen MJ, Donald AE, Seymour CA, Deanfield JE *Cholesterol and arterial distensibility in the first decade of life: a population-based stud.* Circulation 2000: 101:1533-1538.
4. Chrife R, P.V., Spodick DH *Measurement of the left ventricular ejection by digital plethysmography.* American Heart Journal, 1971(82:222-227).
5. Kelly RP, H.C., Avolio AP, O'Rourke MF, *Noninvasive determination of age-related changes in the human arterial pulse.* Circulation, 1989: 80:1652-1659.
6. O'Rourke MF, K.R., Avolio AP, *The arterial pulse.* Philadelphia : Lea & Febiger, 1992: 3-14.
7. Darne BM, G.X., Safar ME, Cambien FA, Guize L *Pulsatile versus steady component of blood pressure. A cross-sectional and prospective analysis on cardiovascular mortality.* Hypertension, 1989: 13:392-400.
8. Kelly RP, H.C., Kerber S, Vielhauer C, Hoeks AP, Zidek W, Rahn KH, *Different effects of hypertension, atherosclerosis and hyperlipidemia on arterial distensibility.* Hypertension, 1995: 13:1712-1717.
9. Takazawa K, T.N., Fujita M, Matsuoka O, Saiki T, Aikawa M, Tamura S, Ibukiyama C, *Assessment of vascular agents and vascular aging by the second derivative of photoplethysmogram waveform.* Hypertension, 1998: 32:365-370.
10. Bortolotto LA, B.J., Kondo T, Takazawa K, Safar ME *Assessment of vascular aging and atherosclerosis in hyperetensive subjects: second derivative of photoplethysmogram versus pulse wave velocity.* . Hypertension 2000: 13:165-171.
11. Elgendi, M., *Standard Terminologies for Photoplethysmogram Signals.* Current Cardiology Reviews, 2012; **8**(3): 215-219.
12. Fitchett, D.H., *Forearm arterial compliance: a new measure of arterial compliance?* . Cardiovascular Research, 1984: 18:651-656.
13. Seki, H., *Classification of wave contour by first and second derivative of plethysmogram (in Japanese).* Pulse Wave, 1977: 7:42-50.
14. Ozawa, T., *Pattern of second derivative of volume pulse wave, the relation between non-invasive index of ventricular function and peak acceleration and effect of preloading to peak velocity (in Japanese).* Pulse Wave 1978: 8:22-31.
15. Elgendi, M., *On the Analysis of Fingertip Photoplethysmogram Signals.* Current Cardiology Reviews, 2012; **8**(1): 14-25.
16. Takazawa K, F.M., Kiyoshi Y, Sakai T, Kobayashi T, Maeda K, Yamashita Y, Hase M, Ibukiyama C, *Clinical usefulness of the second derivative of a plethysmogram (acceleration plethysmogram).* Cardiology, 1993: 23:207-217.
17. Takada H, W.K., Harrel JS, Iwata H *Acceleration plethysmography to evaluate aging effect in cardiovascular system. Using new criteria of four wave patterns.* . Medical Progress through Technology, 1996: 21:205-210.
18. Imanaga I, H.H., Koyanagi S, Tanaka K *Correlation between wave components of the second derivative of plethysmogram and arterial distensibility.* Jpn Heart J 1998: 39:775-784.
19. Takazawa K, T.N., Fujita M, Matsuoka O, Saiki T, Aikawa M, Tamura S, Ibukiyama C, *Assessment of vasocative agents and vascular aging by the second derivative of photoplethysmogram waveform.* Hypertension, 1998: 32:365-370.

20. Nousou, N., Urase, S., Maniwa, Y., Fujimura, K., and Fukui, Y., *Classification of Acceleration Plethysmogram Using Self-Organizing Map*. Intelligent Signal Processing and Communications, 2006. ISPACS '06. International Symposium on, 2006: 681-684.
21. Baek, H.J., Kim, J.S., Kim, Y.S., Lee, H.B., and Park, K.S., *Second Derivative of Photoplethysmography for Estimating Vascular Aging*, in *The 6th International Special Topic Conference on Information Technology Applications in Biomedicine*, 2007.
22. Kimura, Y., Takamatsu, K., Fujii, A., Suzuki, M., Chikada, N., Tanada, R., Kume, Y., and Sato, H., *Kampo therapy for premenstrual syndrome: Efficacy of Kamishoyosan quantified using the second derivative of the fingertip photoplethysmogram*. Japan Society of Obstetrics and Gynecology, 2007.
23. Homma, S., Ito, S., Koto, T., and Ikegami, H., *Relationship between accelerated plethysmogram, blood pressure and anterior elasticity*. The Japanese Society of Physical Fitness and Sport Medicine, 1992; **41**: 98-107.
24. Ushiroyama, T., Kajimoto, Y., Sakuma, K., and Ueki, M., *Assessment of chilly sensation in Japanese women with Laser Doppler Fluxmetry and Acceleration Plethysmogram with Respect to Peripheral Circulation*. Bulletin of the Osaka Medical College, 2005; **51**(2): 76-84.
25. Sano, Y., *Kasokudo Myakuha ni kansuru Kenkyuu no Gaiyou (in Japanese)*, 2003: <http://jsspot.org/sano/>.
26. Matsuyama, A., *ECG and APG Signal Analysis during Exercise in a Hot Environment*, in *School of Engineering and Information Technology*, 2009; Charles Darwin University: Darwin, Australia.
27. Friesen, G.M., Jannett, T.C., Jadallah, M.A., Yates, S.L., Quint, S.R., and Nagle, H.T., *A comparison of the noise sensitivity of nine QRS detection algorithms*. Biomedical Engineering, IEEE Transactions on, 1990; **37**(1): 85-98.
28. Oppenheim, A. and Shafer, R., (eds). *Discrete-time Signal Processing* NJ: Prentice Hall; 1989.
29. Elgendi, M., Jonkman, M., and De Boer, F. *Measurement of a-a Intervals at Rest in the Second Derivative Plethysmogram*. Proceedings of IEEE Conference in Bioelectronics and Bioinformatics, 2009; RMIT University, Melbourne.
30. Elgendi, M., Jonkman, M., and De Boer, F. *Heart Rate Variability Measurement Using the Second Derivative Photoplethysmogram*. Proceedings of The 3rd International Conference on Bio-inspired Systems and Signal Processing (BIOSIGNALS2010), 2010; Spain.
31. Elgendi, M., Jonkman, M., and De Boer, F., *Heart Rate Variability and Acceleration Plethysmogram measured at rest*, in *Biomedical Engineering Systems and Technologies*, A. Fred, J. Filipe, and h. Gamboa, Editors. 2011, Springer. p. 266-277.
32. Elgendi, M., Jonkman, M., and De Boer, F. *Applying the APG to measure Heart Rate Variability*. Proceedings of The 2nd International Conference on Computer and Automation Engineering, 2010; Singapore.